

An Outlook of Medical Image Analysis via Transfer Learning Approaches

Mallela Siva Nagaraju, Battula Srinivasa Rao*

School of Computer Science and Engineering, VIT-AP University, Andhra Pradesh 522237, India

Corresponding Author Email: srinivas.battula@vitap.ac.in

<https://doi.org/10.18280/ts.390502>

Received: 17 August 2022

Accepted: 2 October 2022

Keywords:

histopathology images, visualization techniques, GradCam, SmoothGard, deep learning models, image processing techniques

ABSTRACT

Artificial intelligence advancements, particularly deep learning algorithms, are helpful for identifying, classifying, and rating designs in clinical images. Clinical diagnosis and scientific research both rely heavily on medical image analysis. The diagnosis of medical conditions frequently involves medical image acquisition techniques like pathology, computed tomography, magnetic resonance imaging, ultrasound, and x-ray. Transfer learning stands out from other deep learning techniques thanks to its simplicity, effectiveness, affordable training costs, and capacity to escape the dataset curse. The diagnosis of anomalies including Alzheimer's disease, diabetic retinopathy, colon cancer, breast cancer, and pulmonary nodule can be made using the medical imaging techniques combined with datasets and computer vision. These approaches are helpful in non-invasive qualitative and quantitative analysis on patients. However, labelling in medical images are still scarce. This paper mainly reviews the application of transfer learning in medical image analysis. Beginners can benefit from this review paper's guidance as they gain a thorough and organized understanding of transfer learning applications for the analysis of medical images. By establishing laws that will aid future advancements in medical image processing, policymakers in adjacent sectors will also profit from the trend of transfer learning in medical imaging.

1. INTRODUCTION

Around 2006, a division of machine learning known as deep learning first emerged. It is an approach to handle information that makes use of numerous levels of confusing designs or various handling layers made out of distinct nonlinear alterations [1]. Deep learning has recently made substantial strides in the fields of bioinformatics, computer vision, speech recognition, natural language processing, and audio recognition. Thanks to its application potential in information evaluation, deep learning was recognized as one of the top ten technological discoveries of 2013 [2]. As an artificial neural network, deep learning mimics the human neural network. Layer by layer, the data is preoccupied with numerous nonlinear dealing layers and various levels of unique features extracted from the data for target detection, order, and division [3]. By using unsupervised or semi-supervised feature learning and effective hierarchical feature extraction methods, deep learning reduces the necessity for manual element security.

The goal of medicinal science is to improve people's health and quality of life. As a result, medicine has always been regarded as one of the highest-regarded specialties in the world [4]. Medical research relies heavily on clinical image analysis. Modern clinical investigation in research centers and clinical discoveries need a lot of evidence supported by medical image analysis in order to make a guess or a determination [5]. These safe imaging procedures take into account both an emotional and a quantitative evaluation of incidental effects at the sensitive spot and are generally safe for the patient's body. They have been applied to the brain, heart, colon, eyes, chest, lung, kidney, and liver, among other basic organs [6]. For

medical image analysis using artificial intelligence, a skilled physician is more than necessary. The problem is that finding experts who can perform medical image analysis is exceedingly difficult [7].

Recently, a growing number of researchers have confirmed that, in their testing, convolutional neural network-based clinical image evaluation systems outperformed humans in some clinical imaging illuminating records in terms of correctness. Medical images are notoriously expensive, difficult to get, and in short supply [8]. Additionally, the rarity of tagged data is increased by the fact that only licensed physicians can label medical images. These factors have caused convolutional neural networks to make poor progress in the analysis of medical images.

In this research, deep learning algorithms for medical image analysis are introduced first, followed by deep learning techniques for classification and segmentation, and finally, more traditional and up-to-date mainstream network models [9]. It will be useful for image segmentation and classification in digital pathology, CT/MRI tomography, ultrasound, and fundus imaging. The work also considers potential problems and makes predictions about the direction of deep learning in medical imaging analysis.

2. ADVANCEMENT OF CONVOLUTIONAL NEURAL NETWORK

In recent years, deep learning has shown undeniable proficiency in the area of medical image processing. Convolution neural network (CNN) is one of the most

established and widely used deep learning techniques in the processing of medical images [10]. Higher accuracy is achieved by CNN compared to earlier image classification techniques, laying the basis for transfer learning-based image processing [11-13]. There is minimal likelihood of transfer learning in the realm of medical image processing unless and until CNN is created and enhanced [14]. In fact, many transfer learning techniques are built around CNN. In recent years, one of the most common transfer learning techniques is to use pre-trained CNN models, freeze some layers, and then retrain some layers using data from the target area [15]. Most pre-trained transfer learning models, including AlexNet, VGGNet, and ResNet, among others, adopt CNNs. Without carefully examining CNNs, it is challenging to comprehend all aspects of current transfer learning strategies [16]. Understanding CNN architecture, optimization techniques, and representative CNN models is essential for comprehending transfer learning in medical imaging [17].

The convolutional parameters are usually defined as follows: K is the bit size, T is the original image size, P is the zero-cushioning, S is the step, and U is the size of the output feature map. Each portion can be described as an element extractor of the size of a K×K grid. For simplicity, the original image and output feature map are assumed to have T×T pixels and U×U pixels, respectively. Cushioning is every now and again used to enhance additional pixels of significant worth zero around the original image, such that CNN arrives at the expected distance. In this case, the size U of the output feature map can be expressed as:

$$U = T - K + 1 \tag{1}$$

The convolution has no padding, with a stride of one. To accommodate more complex scenarios, a zero-padding circle should be added around the input image. Then, the above formula can be revised as:

$$U = T - K + 2p + 1 \tag{2}$$

2.1 Pooling

From the input image, the convolutional layer extracts a sufficient number of features. Multi-features, however, may not always be a good thing. Only essential feature information is kept when the pooling layer down samples extracted feature maps and reduces feature map resolution [18]. The neural networks can have fewer parameters because this layer conducts convolution operations on its set parameters. Translation invariance aids in this layer's performance. There are two distinct pooling methods: max pooling and average pooling. Max pooling chooses the highest value possible from an image's local domain to better preserve the image properties. Average pooling takes the average value from a local domain inside an image for the same purpose. Max pooling and average pooling are convolutions that stride the same number of pixels as their kernels [19].

2.2 Fully connected layer

The convolution process creates a fully connected layer using the feature maps after the convolution, pooling, and activation. This layer employs convolution kernels to perform convolution on feature maps in order to obtain a one-layered vector. The objective is to reduce the spatial dimension of the

neural network while weighting all of its attributes. Using softmax simplifies the output of classification probability output. A fully connected network in a conventional CNN is often constructed using multiple neural networks [20]. A sizeable chunk of the entire CNN is made up of its parameters. When the fully connected layer has too many parameters, overfitting takes place. The average pooling can be directly applied to the entire feature space. By producing a single-layered vector, this operation effectively reduces the number of boundaries in the model. Global normal pooling does not, however, always outperform the fully connected layer in machine learning. There is more customization because the majority of boundaries are remembered for a fully connected layer.

2.3 Batch normalization

Deep learning network tuning is difficult and frequently leads to internal covariate shift. When network parameters change, internal nodes' data distribution shifts. There are two main effects of the shift. One is that the upper network's learning rate is decreased because it must constantly adapt to changes in the distribution of input data. Second, network convergence is slowed down for the activation function enters the gradient saturation zone [21]. Batch normalization provides an efficient way to transform an output signal into an optimum range. Given a set of input from a single neural network layer, we have:

$$X = [x_1, x_2, x_3, \dots, x_n] \tag{3}$$

where, x_i is the number of samples; n is the batch size. Firstly, compute the mean of the mini-batch elements:

$$\varphi_B = \frac{1}{n} \sum_{i=1}^n x_i \tag{4}$$

Secondly, compute the variance of the mini-batch elements:

$$w^2_B = \frac{1}{n} \sum_{i=1}^n (x_i - \varphi_B)^2 \tag{5}$$

Then, normalize each element from the mini-batch:

$$x^1_i = \frac{x_i - \varphi_B}{\sqrt{w^2_B + \epsilon}} \tag{6}$$

The original output must be scaled and shifted to account for the nonlinear expression of the network.

Batch normalization has the advantage of making sure the data entered into each network layer is within a range. Layer decoupling, which enables accelerating learning of the entire brain organization, results from the following layer network not having to constantly obey changes in the basic layer of the organization. The model's aversion to organizational boundaries is reduced by batch normalization, which also increases the network's adaptability to boundary ranges and the stability of organizational learning. The vanishing gradient problem can be solved by reducing the impact of changes in the hidden organization collecting with the top organization and preventing the enactment capability from accessing the angle immersion zone during training [22]. Finally, irregular

commotion is introduced into the organizational learning process, resulting in some degree of regularization.

2.4 Dropout

Deep learning is powerless to overfitting. Even with minimal training data, the network and its boundaries can grow large and complex, which would bring overfitting. Dropout hence takes up the majority of the time during deep neural network preparation. Overfitting is less of a problem thanks to setting the hidden layer's portion of the hubs to 0, which is equivalent to ignoring a portion of the component identifiers by random [23].

2.5 Regularization

Regularization, in addition to dropout, is a typical approach to handle overfitting. It happens when some hidden layer node parameters are overtrained, which has a negative effect on the overall model prediction outcomes. When an organization prepares information very closely to the truth, it makes crucial errors when testing that information. This can be avoided by using strategies like early stopping, sampling, and increasing the learning rate [24].

3. TRANSFER LEARNING

In the realm of clinical imaging, a single circumstance is typical. The availability of sample data is typically limited because creating a data set is laborious and expensive. Moreover, after learning some new useful information from a previous problem, we must immediately move on to the next task. Transfer learning is extremely important because of this. The target area is new information, while the source area is information that already exists. Before providing a standard definition of transfer learning, two fundamental concepts should first be characterized [25]: Include space X and minimal conveyance P make up the two sections of an area, which is denoted by the letter D . (X). In this case, the area can be defined as:

$$D = \{X, P(X)\} \tag{7}$$

Each task T can be defined using the definition of domain.

$$T = \{\gamma, P(Y|X)\} \tag{8}$$

$P(Y|X)$ is a function that predicts the corresponding label

based on feature space. We now have a task specification as a result.

$$T = \{\gamma, \eta\} \tag{9}$$

The basic architecture of transfer learning is shown in Figure 1. There is a source area D and its matching task T , as well as a target area DT and its critical task TT . Either $D_s \neq DT$ or $T_s \neq TT$. In each cycle, it is necessary to obtain the objective probability for a task ηT in DT using the data acquired from D_s and T_s .

3.1 Instance-based transfer learning

The instance-based transfer learning process is straightforward and unambiguous. The data that resembles those in the source space and target region should be marked and given even more weight, after looking at the source and target regions. This process is equivalent to selecting the information from the source space that is closest to the information in the target area, then matching the objective domain at that point [26]. This method's drawbacks include being more erratic, observational, and lacking a consistent subset of data in the source space that is extraordinarily close to the target area.

3.2 Feature-based transfer learning

The target area and source area are thought to share some covering features, which is the underlying assumption for feature-based transfer learning. Through highlight transformation, the source and target areas can then be combined into a single space [27]. When the source area and the target area are in close proximity, their information will circulate similarly. As a result, we can use AI to complete the remaining tasks. Feature -based move learning has the advantage that, despite occasionally being difficult to determine, it performs relatively well.

3.3 Relationship-based transfer learning

Relationship-based transfer learning raises questions about whether the source and target areas are sufficiently similar to provide a real relationship or something resembling one. The task of moving knowledgeable relationships from the source area to the target area is at the heart of connection-based move gaining [28-32]. Table 1 summarizes the four transfer learning mechanisms.

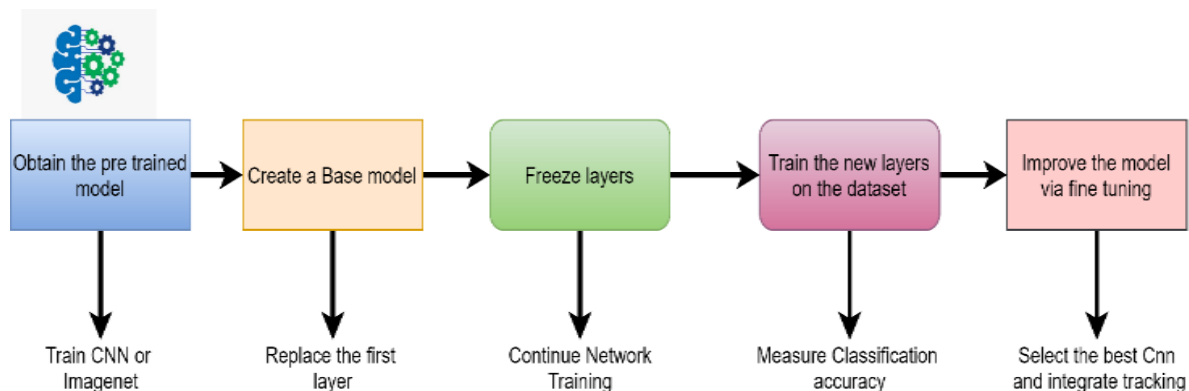


Figure 1. Basic architecture of transfer learning

Table 1. Different transfer learning approaches

Type	Process	Features
Instance-based transfer learning	Utilize target data in a source area instance.	Suitable for direct reusing data from the source area
Feature-based transfer learning	Utilize feature representation from the source area, and represent features in the target area.	Reducing the gap between the source and target areas, but mostly rely on labelled data
Parameter-based transfer learning	Compensate for loss in the target area during re-training, and use parameters from the source area for initialization and weighting.	Using a pre-trained model rather than starting from scratch, making training new neural networks much faster
Relationship-based transfer learning	Discover the relationship between data points in the source area.	Compatible with the data that are dependent on each other and have the same distribution

3.4 MobileNetV2

The CNN architecture called MobileNetV2 (Figure 2) has been enhanced for mobile devices. It depends on the remaining connections between the bottleneck levels in the revised residual structure. The average development layer adds nonlinearity by combining lightweight profundity wise convolutions with highlights [33]. In terms of engineering, MobileNetV2 normally uses a 32-channel fully convolution layer at the beginning, followed by 19 residual bottleneck layers.

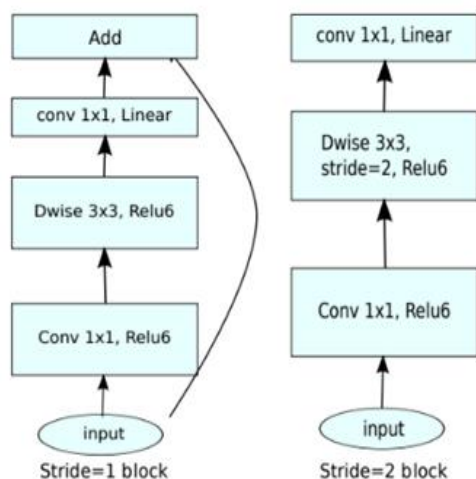


Figure 2. Architecture of MobileNetV2

3.5 Inception-ResNet-v2

A convolutional brain network called Inception-ResNet-v2 (Figure 3) was constructed utilizing more than 1,000,000 images from the ImageNet dataset. The 164-layer structure can be broken down into 1,000 different item classes, including those for the console, mouse, pencil, and many different animals. The organization consequently learned specific component depictions for a wide range of images [34]. The organization receives a 299×299 image and provides a list of

estimated class probabilities. Both the Inception structure and the Residual connection influence the performance of this network. The Inception-ResNet block joins numerous calculated convolutional channels and residual relationships. Utilizing existing connections not only avoids the debasement problem that extensive designs bring about, but also shortens the preparation period.

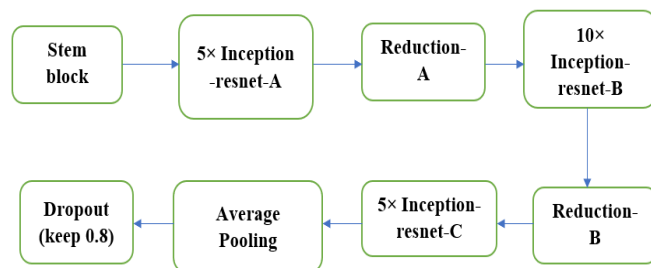


Figure 3. Architecture of InceptionResNetV2

3.6 DenseNet

In a traditional feedforward CNN, each convolutional layer—aside from the first, which receives input—receives the output of the layer before it and produces a feature map, which is then passed on to the next convolutional layer. There are then "L" direct relationships between every layer and the layer following the "L" layers. However, as the CNN's layer count grows, the vanishing gradients problem manifests itself. This actually means that some data may "disappear" or be lost when the data path to the result layers lengthens, making it harder for the organization to plan effectively [35]. DenseNet (Figure 4) takes care of this issue by adjusting the standard CNN design and working on the layer network design. In the DenseNet, each layer is straightforwardly associated with each and every other layer. For L layers, there exist $L(L+1)/2$ direct connections.

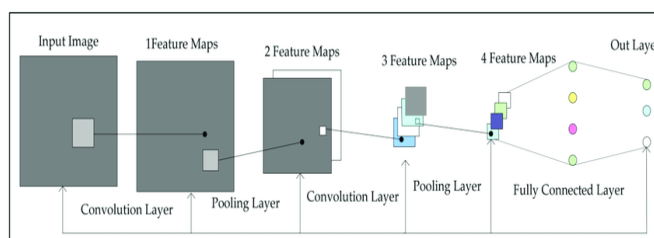


Figure 4. Basic architecture of DenseNet

3.7 ResNet

Image processing and identification have advanced significantly in recent years. Deep neural networks are developing into increasingly sophisticated and complex systems. It has been shown that a neural network's robustness for image-related tasks is improved by layering the network. But it is probable they will lose precision in the process. This is where residual network (Figure 5) can help. Deep learning experts frequently build numerous layers to extract important information from complex images [20, 36]. As a result, the first layers may differentiate edges, and the last layers may do the same for obvious forms like car tires. However, adding more than 30 levels to the organization degrades its precision and display.

Table 2. Deep learning models for medical image analysis

Authors	Focus	Remarks
Ker et al. [37]	Medical images are analyzed based on classification and segmentation.	Describing the utilization of different managed and solo deep learning models on clinical images
Litjens et al. [38]	Most articles focus on the classification, segmentation and analysis of medical images using deep learning.	Reporting a series of deep learning methods and their applications to clinical imaging undertakings
Mazurowski et al. [39]	This is a review of the use of profound learning in radiology, focusing on grouping and division.	Image classification tasks using transfer learning strategies and deep features
Pehrson et al. [40]	Deep learning techniques were used to detect pulmonary nodules in lung images.	No mention of transfer learning strategies
Sengupta et al. [41]	This is a review of medical image processing using deep learning architectures and application.	Theoretical and mathematical explanation of CNN application in power systems
Shorten and Khoshgoftaar [42]	This work introduces different data augmentation approaches.	Building taxonomy for image data augmentation
Yi et al. [43]	This a review of medical image analysis and a comprehensive overview of GAN.	Reviewing GAN application with medical images but not transfer learning strategies
Zhuang et al. [44]	Current transfer learning approaches are reviewed and summarized, with a focus on data and models.	Providing examples of natural language processing (NLP)
Wang et al. [45]	This is an introduction to the articles distributed between 2000 and 2020.	Explaining how to use medical images for scientific research and clinical diagnosis.
Shinde et al. [46]	This work details all transfer learning designs and methodologies.	Examining various award-winning transfer learning architectures, as well as their application to various medical imaging resources
Xie et al. [47]	This work provides a concise outline of the benchmark clinical image datasets.	Shedding light on the ongoing circumstance and difficulties
Wang et al. [48]	This is a review of Transfer learning techniques for health monitoring.	Inspiring ground-breaking thoughts for working with medical care

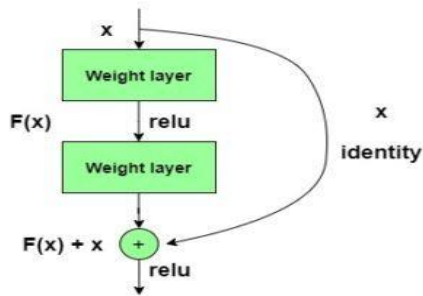


Figure 5. Basic architecture of ResNet

$$y = F(x) + x \quad (10)$$

The ResNet152 model with 152 layers won the ILSVRC ImageNet 2015 test, despite having fewer boundaries than the established VGG19 network at that time. A lingering

network is composed of residual units or blocks that are linked by personality connections, also known as skip connections. Table 2 summarizes the various deep learning models applied to medical images.

4. MEDICAL IMAGE APPLICATIONS

As common deep learning technique, transfer learning allows a model created for one task to be utilized as the starting point for another related model. This technique guarantees time and resource optimization, while improving the effectiveness and performance of the pretrained deep learning models. For an effective analysis of medical images, the transfer learning techniques have been adopted for the abnormalities of Alzheimer's disease, diabetic retinopathy, colon cancer, breast cancer, and pulmonary nodule, as shown in Table 3.

Table 3. Transfer learning approaches for disease detection with medical image analysis

References	TL_Approaches	Disease	Remarks
Wang and Zhang [49]	VGG_inspired network	Alzheimer's disease	Classification of Alzheimer's disease
Acharya et al. [50]	InceptionV3	Alzheimer's disease	MRI scan of Alzheimer's disease
Wang et al. [51]	DenseNet	Alzheimer's disease	Detecting various sclerosis diseases
Swati et al. [52]	VGG19	Brain Tumor	Classification of brain tumors in MR images via transfer learning
Lao et al. [53]	CNNS	Alzheimer's disease	GBM detection and classification of MRI images
Puranik et al. [54]	Inception-V2 and Finetuning	Alzheimer's disease	Detection of Alzheimer's disease
Cheng et al. [55]	Feature extractor	Alzheimer's disease	Classification of Alzheimer's disease
Lu et al. [56]	Fine-tuning on AlexNet	Alzheimer's disease	Pathological brain detection

Sathananthavathi and Indumathi [57]	U-Net	Diabetic retinopathy	Segmentation of diabetic retinopathy images
Raju and Rao [58]	Inception V3	Diabetic retinopathy	Diabetic retinopathy detection using fundus images
Chen et al. [59]	GoogleNet	Diabetic retinopathy	Diabetic macular edema identification
Suan et al. [60]	VGG,Googlenet,AlexNet	Diabetic retinopathy	Classification of diabetic retinal images
Motozawa et al. [61]	Custom_CNN	Diabetic retinopathy	Detection of age-related macular degeneration
Valerio et al. [62]	Inception V3, InceptionResNet-v2 and NASNetLarge	Breast cancer	Mammography for breast lesion detection
Moroianu and Rusu [63]	VGG19	Breast cancer	MRI-based diagnosis of breast cancer
Mendel et al. [64]	AlexNet,CNN	Breast cancer	Mammogram for breast lesion detection
Aljuaid et al. [65]	ResNet 18, ShuffleNet, and Inception-V3Net	Breast cancer	Breast cancer detection with multitask transfer learning
Islam et al. [66]	ResNet50	Breast cancer	Breast lesion detection using ultrasound images
Byra et al. [67]	Inception-V3, VGG19 and InceptionResNetV2	Breast cancer	Breast lesion classification using transfer learning
Li et al. [68]	DenseNet with SENet (IDSNet)	Breast cancer	Breast cancer detection using histopathology images
Gessert et al. [69]	Inception-V3 and Densenet121	Colon cancer	Classification of colon cancer using microscopic images
Dulf et al. [70]	Googlenet and AlexNet	Colon cancer	Detection of colon polyp
Raju et al. [71]	Modified ResNet150	Colon cancer	Classification of colon cancer
Kang and Gwak [72]	ResNet50 and ResNet101	Colon cancer	Polyp instance segmentation using Mask-RCNN
Zhang et al. [73]	ResNet18 and ResNet50	Colon cancer	Detection of colon cancer
Xiong et al. [74]	LeNet-5 and AlexNet	Pulmonary nodule	Classifying pulmonary nodules from CT images via transfer learning
Hussein et al. [75]	ResNet101	Pulmonary nodule	Identification of lung adenocarcinom
Zhang et al. [76]	DeepNN	Pulmonary nodule	Discovering lung nodules and pancreatic cysts
da Nóbrega et al. [77]	Custom CNN	Pulmonary nodule	Screening of tuberculosis disease
Bassi and Attux [78]	ResNet50	Pulmonary nodule	Lung nodule classification using CT images

4.1 Detection of Alzheimer's disease

A basal ganglia problem that causes a steady deterioration in motor accuracy and sensor motor integration is the hallmark of the neurological condition known as Alzheimer's disease. Scale and shift invariant characteristics, including data shape, mean, and standard deviation, are employed by Wu et al. [79] to conduct classification on functional MRI using a CNN model. The suggested fMRI system was trained on 27000 images before being validated and evaluated on 9000 images. The authors' accuracy in identifying brains affected by Alzheimer's disease was 92.86 percent. In 3D patches of MRI and PET scans, ecomist et al. [80] employed the deep Boltzmann machine (DBM) to extract features and find anomalies. With accuracies of up to 92.38 percent, 92.20 percent, and 94.35 percent, the results were validated using PET, MRI, and a combination of the two on the ADNI dataset for Alzheimer's disease.

Hassaballah and Awad [81] investigated the use of 3D-CNN for the diagnosis of Alzheimer's disease and retrieved standardized features from the CAD Dementia MRI dataset. After that, the authors improved three fully connected layers of CNN for the categorization of Alzheimer's disease using the ADNI dataset. Ciaparrone et al. [82] used MRI and fMRI scans to identify adult cases of Alzheimer's disease (over the age of 75). The researchers conducted both research and clinical application investigations. The CNN model demonstrated 96.9% accuracy for functional MRI data and

95.84% accuracy for MRI data in the detection of normal or Alzheimer's brain. They subsequently created a decision-making system employing classification at the subject level.

With the use of a sparse auto encoder (a neural network), Elharrouss et al. [83] retrieved features from an ADNI dataset of neuron images, and adopted 3D-CNN subsequently as a classifier. The accuracy ranged from 95.39 percent for Alzheimer's disease to 95.39 percent, after the dataset was split into three sections: training (1,731 samples), validation (306 samples), and test (228 samples). Prior to dividing Alzheimer's brains into prodromal and mild cases, Liu et al. used a sparse auto encoder to extract generic features. Using binary MRI and PET images, they detected early-stage Alzheimer's disease with an accuracy of 87.76%.

4.2 Diabetic retinopathy

High glucose levels are caused by diabetes mellitus, a metabolic disorder in which the body's cells do not respond to insulin 2 or the pancreas does not produce enough of it. A diabetic eye condition that can impair vision is diabetic retinopathy. According to estimates, diabetes affects over 415 million people worldwide, with 15% being at high risk for vision impairment, blindness, or other misfortune. If detected early via a retinal screening test, it is successfully curable and manageable. Physically identifying diabetic retinopathy is a difficult and time-consuming process due to a lack of equipment and expertise. Since there are not many early-stage

side effects of this illness, treatment is put off, misunderstandings arise, and follow-ups are missed. Instead, a doctor should examine the darkened fundus image of the retina.

Deep learning models have been discovered to be more accurate and improved at detecting diabetic retinopathy. This section summarizes the profound learning techniques applied to the treatment of diabetic retinopathy.

To organize and distinguish between moderate and bad referable on datasets from the Eye Image Archive Communication System (EyePACS-1) and Messidor-2, Shankar et al. [84] utilized deep convolutional neural network (DCNN). Around 10,000 retinal images may be found in the EyePACS-1 informational index, whereas 1,700 retinal images from 874 individuals can be found in the Messidor-2 informational index. According to the developers, EyePACS-1 is 97.5 percent sensitive and 93.4 percent explicit, whereas Messidor-1 is 96.1 percent aware and 93.9 percent particular.

Using dropout layer techniques, Li et al. [85] prepared a DCNN for fundus arrangement and tested on openly available datasets including kaggle fundus, DRIVE, and STARE. The accuracy was found to range between 94 and 96 percent. Over 80,000 digital fundus images from the Kaggle dataset were utilized, along with the NVIDIA CUDA DCNN library. They used 5,000 images to test the network as well. The images were cropped to 512x512 pixels and sharpened. The Cu-DCNN was then given the feature vector. By classifying the images into five groups based on exudates, hemorrhages, and microaneurysms, the proposed method was able to obtain up to 95 percent specificity, 30 percent sensitivity, and 75 percent accuracy.

4.3 Detection of colon disease

All organs associated with food processing, supplement retention and waste discharge are remembered for the gastrointestinal (GI) plot. It starts with the mouth and advances to the butt. Among the organs are the throat, stomach, internal organ (colon or enormous inside) and small digestive system (little entrail). Upper and lower GI parcels can be recognized too. The upper GI parcel comprises of the throat, stomach and duodenum (part of the little inside), while the lower GI lot comprises of most of the small digestive tract and internal organ. Food assimilation and retention are hampered by aggravation, dying, diseases and cancer. Ulcers cause upper gastrointestinal dying. Polyps, disease and diverticulitis are likely reasons for colon dying. The small intestine is affected by diseases such celiac disease, Crohn's disease, both malignant and benign tumors, gastrointestinal obstructions, duodenal ulcers, irritable bowel syndrome, and drainage caused by arteriovenous mutations.

Image handling and AI are fundamental to identifying and analyzing these diseases, enabling medical professionals to seek appropriate and accurate therapeutic options. Different imaging tests are now used to diagnose and place stomach-related framework illnesses as computer aided design (CAD) frameworks advance. Among the imaging procedures available are remote case endoscopy, endoscopy and enteroscopy, colonoscopy or sigmoidoscopy, radiopaque colors and X-ray review, profound little gut endoscopy, intraoperative enteroscopy, computed tomography, and MRI.

In GI 10,000 WCE images, draining was identified using DCNN. The WCE is a painless video image assessment technique for internal infections that are not severe. Focusing on width examples and gut length using global data, Cheng et

al. [55] created fully convolutional networks (FCN) and layered them with LSTM using small and large datasets. The FCN framework was applied to a large dataset of fifty unmarked, unprocessed crude cine MRI groupings, while the FCN-LSTM was developed on a small dataset of five unprocessed crude cine MRI successions. Gaining details from the ImageNet dataset was handled into CNN SoftMax for ordering and identifying celiac disease using duodenum endoscopic images. CNN is a well-known method for extracting programmed highlights from endoscopic images [38]. The elements vector is then utilized to describe and identify gastrointestinal injuries using the SVM. On 180 images, the suggested framework for sore discovery was tested, and a precision of 80% was achieved. Merjulah and Chandra [5] likewise utilized a mixture system.

Dulf et al. [70] used CNN design to quickly extract components. The extracted highlights were then sent to SVM for detection of provocative gastrointestinal disease in WCE recordings. The tests were conducted on 599 non-friery images and 337 explained incendiary images from KID's GI plot. There was a general exactness of up to 90% between the test set's 27 typical and 27 strange samples and the preparation set's 200 ordinary and 200 extraordinary examples. Colonoscopy recordings of polyps were discovered using three alternative image representations. To improve the accuracy of polyp limitation, various CNN models were created on disconnected aspects such as surface, form, variety, and global data at various scales. The results were then combined to make a final decision. In comparison to cutting-edge methods, the researchers claimed that their polyp dataset reduces polyp detection idleness and is the largest commented-on dataset.

Additionally, Phillips et al. [32] conducted three tests using various CNN coupled with standardization. The amount of the dataset increased as a result of information expansion by producing various image types. They carried out another investigation using CNN and pixels to organize polyp growth with colonic mucosa as a target feature.

4.4 Ultrasound detection of breast nodules

Research breakthroughs in areas including cardiovascular disease, carotid supply routes, and bosom malignant growth have been made thanks to deep learning innovation. In contrast to traditional AI, deep learning may make use of multifaceted models to organically channel features to improve recognition performance. Due to its great accuracy and precision, which may primarily be used for indicative precision, deep learning has evolved into an important tool for ultrasonic image recognition. When surface elements and morphology identification techniques were combined in the field of ultrasound imaging of breast knobs, using the AlexNet model to locate the knobs in the image and predict the benign and dangerous, the AUC esteem was solidified and reached 0.9325.

Mendel et al. [64] resorted to deep learning to improve the division impact of the left ventricular ultrasound image of the heart. On the preset sequence of fetal face ultrasound images, 96.98% accuracy was achieved using CNN and an irregular two-coordinate drop streamlining calculation (28). Deep conglomeration highlights are used in conjunction with the ResNet model to detect melanoma in thermoscopic images. The AUC, which is more than 80%. suggests the grouping of bosom knobs information preprocessing upgrade can be realized using the versatile differentiation improvement (ACE) technique. The results are frequently subpar when the first

input is transmitted directly to the brain network. The ultrasound image is then further developed using the ACE calculation [65, 66]. By calculating the general pixel value of the objective point and encompassing pixels by distinction, the ACE computation may be applied to the images.

4.5 Screening of pulmonary nodule

The most well-known type of lung infection is pneumoconiosis. Figure 6 shows a complete CT image of a pneumonic knob. Even people with typical chest films can be identified to have sarcoidosis due to the low symptomatic accuracy of normal X-beam chest films in the identification of pneumonic knobs. Cellular breakdown in the lung screening and identification is being remembered for an increasing number of physical tests as CT becomes the primary method for pneumonic knob diagnosis. According to information measurements, the pneumonic knob's recognition rate has recently increased fivefold.

As deep learning technology advances, various profound learning techniques for differentiating pneumonic knobs are emerging. They evaluated a few different lung knob recognition methods and discovered that, in terms of knob discovery rate, the deep learning calculation outperformed the conventional AI calculation. However, the deep learning algorithm is limited in its ability to distinguish aspiratory knobs. To begin with, the accuracy of the comment data and the numerous informational collections are both impacted by the rapid pace of lung knob recognition [72]. Second, the precision rate decreases as the number of organizational levels increases, indicating that the calculation for profound learning has a limit. A couple of clinical images are shown in Figure 6.

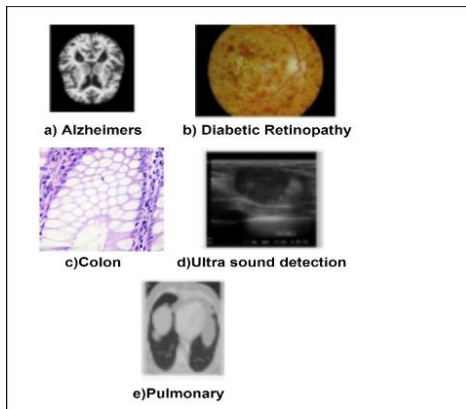


Figure 6. Sample medical images a. Alzheimer’s b. Diabetic Retinopathy c. Colon d. Ultrasound detection breast e. Pulmonary

5. DISCUSSION

As we all know, collecting medical images is always more expensive and challenging than other kinds of vision activities. Furthermore, some medical image capturing techniques are detrimental to patient bodies, which prevents us from gathering a lot of data naturally. We often have very little data in the target area while conducting transfer learning in medical image analysis. There are two main solutions to this problem. First, even though a clinical picture dataset is typically small in size, we may be able to enhance it, which leads us to information expansion technology. Second, while avoiding the

image pool quality requirement, we should use restricted information. Another tactic, smart imaging, aims to change the character of needed images, which is precisely what we need. We will now briefly discuss information expansion and savvy imaging in this section.

5.1 Data augmentation

Fortunately, information increase is a simple yet effective strategy. Information expansion is the process of applying mathematical and photometric adjustments to special images, such as scaling, pivoting, and reflection. In this way, information expansion increases the number of distinct image datasets and promotes their dispersion, bringing it closer to the real world. Data augmentation was a widely used technique that could be seen in a growing number of pertinent studies prior to the acceptance of transfer learning. It is commonly regarded as one of the most efficient and useful strategies for overcoming data shortage.

5.2 Smart imaging

Further, we should emphasize intelligent imaging. Smart imaging is used to obtain image data of higher quality. It might support noise and artifact reduction, shadow detection, and image resolution. Due to all of these factors, deep learning algorithms can deliver results more quickly and accurately.

5.3 Models

In transfer learning, more than simply data and labels are utilized. Models are just as crucial to transfer learning as data and labels. It has a track record of working with and collaborating with other cutting-edge deep learning ideas. In light of this, we shall look at this pattern from three different perspectives. The impact of few shot learning and meta learning theories on transfer learning is the subject of the first query. Next, we will examine the integration of transfer learning with other well-known deep learning models. Third, model interpretability in transfer learning, which may have been disregarded in the past, needs to be addressed.

5.4 Few shot learning and meta learning

As was previously said, performing medical image analysis always results in a lack of samples and labels. In other words, the great majority of medical image processing jobs can be accomplished via few shot learning. The greatest and most effective method for resolving specific learning challenges has been identified as meta learning. Meta learning and motion learning share certain determined and procedural commonalities. In transfer learning, researchers frequently modified an established convolutional mind connection or saw it as a component extractor, then used a variety of classifiers. The three types of meta learning include metric learning, RNN memory-based learning, and intelligent adjustment.

Sorting out a way to align is the first and most common type of meta learning, and it parallels transfer learning in a variety of ways. The learned instatement limit could eventually complete optimal execution when given new tasks after a number of tendency drop stages and two or three shot models. Another approach is to hire a specialist in LSTM-based smoothing out to help with fine-tuning [70]. Many people agree that meta learning uses altering, which is appropriate.

Although there are not many studies on clinical image evaluation that specifically address shoot learning or meta learning at the moment, we realize that this is an example and that moving forward, the concepts of move gaining and meta gaining will converge.

5.5 Combination with other deep learning models

Since experts first employed a pre-built CNN as an element extractor, transfer learning has been associated with other deep learning techniques. As previously stated, antagonistic based solo space variation used a bad network and a training cycle obtained from a generative adversarial network (GAN). It uses deep learning models that are being developed in close proximity to one another. In reality, a few scientists have tried to use the transfer learning system as a learning assist. Despite the lack of clinical imaging in this discipline, we anticipate that more relevant papers will be published sooner rather than later.

5.6 Model interpretability

The final issue is transfer learning's ambiguous translation and variable organization of prepared models. Although a few studies in this area have been published, very few researchers have focused on medical image analysis. We acknowledge that more work needs to be done even though transfer learning has become a platitude. We hope to see more research and writing on the subject in the future.

6. CONCLUSION

In this research piece, we first go over the fundamental examination concerns in the area of medical image analysis as well as the background of transfer learning in this area historically. The essential premise, development, and application of transfer learning are then discussed in relation to convolutional neural networks. Next, we detail the papers on five typical medical imaging analysis fields: the brain, heart, breast, lung, and kidney. Finally, we discuss a few potential mixtures and the ultimate outcome of transfer learning in medical imaging.

We anticipate that in the field of medical image research, innovations like information expansion, self-administered learning, and space transformation will lead to a constant advancement of transfer learning into meta learning. As an alternative, transfer learning combined with support learning, different models, and viable and powerful archetypes produce continuing neural network execution. Some important works might not be included in this article due to the writer's limited knowledge. Anyhow, we are confident that this research article offers a helpful and enlightening perspective on the evolution and trends in transfer learning in the field of medical imaging.

REFERENCES

[1] Du, Y., Zhang, R., Zargari, A., Thai, T.C., Gunderson, C.C., Moxley, K.M., Liu, H., Zheng, B., Qiu, Y.C. (2018). Classification of tumor epithelium and stroma by exploiting image features learned by deep convolutional neural networks. *Annals of Biomedical Engineering*, 46: 1988-1999. <https://doi.org/10.1007/s10439-018-2095-6>

[2] Caravagna, G., Giarratano, Y., Ramazzotti, D., Tomlinson, I., Graham, T.A., Sanguinetti, G., Sottoriva, A. (2018). Detecting repeated cancer evolution from multi-region tumor sequencing data. *Nature Methods*, 15(9): 707-714. <https://doi.org/10.1038/s41592-018-0108-x>

[3] Chen, H., Qi, X., Yu, L., Dou, Q., Qin, J., Heng, P.A. (2017). DCAN: Deep contour-aware networks for object instance segmentation from histology images. *Medical Image Analysis*, 36: 135-146. <https://doi.org/10.1016/j.media.2016.11.004>

[4] Guo, Y., Ashour, A. (2019). Neutrosophic sets in dermoscopic medical image segmentation. *Neutrosophic Set Med Image Anal*, 11(4): 229-243. <https://doi.org/10.1016/B978-0-12-818148-5.00011-4>

[5] Merjulah, R., Chandra, J. (2019). Classification of myocardial ischemia in delayed contrast enhancement using machine learning. *Intell Data Anal Biomed Appl.*, pp. 209-235. <https://doi.org/10.1016/B978-0-12-815553-0.00011-2>

[6] Oliveira, F.P., Tavares, J.M.R. (2014). Medical image registration: A review. *Computer Methods in Biomechanics and Biomedical Engineering*, 17(2): 73-93. <https://doi.org/10.1080/10255842.2012.670855>

[7] Wang, J., Zhang, M. (2020). Deep FLASH: an EFCIENT network for learning-based Medical Image Registration. In: *Proceedings of 2020 IEEE/CVF Conference on Computer Vision and Pattern Recognition (CVPR)*, pp. 4443-4451. <https://doi.org/10.1109/cvpr42600.2020.00450>

[8] Fu, Y., Lei, Y., Wang, T., Curran, W.J., Liu, T., Yang, X. (2020). Deep learning in medical image registration: A review. *Physics in Medicine & Biology*, 65(20): 20TR01. <https://doi.org/10.1088/1361-6560/ab843e>

[9] Haskins, G., Kruger, U., Yan, P. (2020). Deep learning in medical image registration: A survey. *Machine Vision and Applications*, 31(1): 1-18. <https://doi.org/10.1007/s00138-020-01060-x>

[10] De Vos, B.D., Wolterink, J.M., Jong, P.A., Leiner, T., Viergever, M.A., Išgum, I. (2017). ConvNet-based localization of anatomical structures in 3D medical images. *IEEE Trans Med Imaging*, 36(7): 1470-1481. <https://doi.org/10.1109/TMI.2017.2673121>

[11] Sharma, H., Jain, J.S., Bansal, P., Gupta, S. (2020, January). Feature extraction and classification of chest x-ray images using CNN to detect pneumonia. In *2020 10th International Conference on Cloud Computing, Data Science & Engineering (Confluence)*, pp. 227-231. <https://doi.org/10.1109/Confluence47617.2020.9057809>

[12] Hassan, M., Ali, S., Alquhayz, H., Safdar, K. (2020). Developing intelligent medical image modality classification system using deep transfer learning and LDA. *Scientific Reports*, 10(1): 1-14. <https://doi.org/10.1038/s41598-020-69813-2>

[13] Abbas, A., Abdelsamea, M.M., Gaber, M.M. (2021). Classification of COVID-19 in chest X-ray images using DeTraC deep convolutional neural network. *Applied Intelligence*, 51(2): 854-864. <https://doi.org/10.1007/s10489-020-01829-7>

[14] Kowsari, K., Sali, R., Ehsan, L., Adorno, W. (2020). Hierarchical medical image classification, a deep learning approach. *Information*, 11(6): 318-318. <https://doi.org/10.3390/info11060318>

[15] Singh, S.P., Wang, L., Gupta, S., Goli, H., Padmanabhan,

- P., Gulyas, B. (2020). 3D deep learning on medical images: A review. *Sensors*, 20(18): 5097-5097. <https://doi.org/10.3390/s20185097>
- [16] Shen, D., Wu, G., Suk, H.I. (2017). Deep learning in medical image analysis. *Annual Review of Biomedical Engineering*, 19: 221-248. <https://doi.org/10.1146/annurev-bioeng-071516-044442>
- [17] Wang, S.H., Phillips, P., Sui, Y., Liu, B., Yang, M., Cheng, H. (2018). Classification of Alzheimer's disease based on eight-layer convolutional neural network with leaky rectified linear unit and max pooling. *Journal of Medical Systems*, 42(5): 1-11. <https://doi.org/10.1007/s10916-018-0932-7>
- [18] Song, Y., Zheng, S., Li, L., Zhang, X., Zhang, X., Huang, Z., Chen, J., Zhao, H., Jie, Y., Wang, R., Chong, Y., Shen, J., Zha, Y., Yang, Y. (2020). Deep learning enables accurate diagnosis of novel coronavirus (COVID-19) with CT images. *IEEE/ACM Transactions on Computational Biology and Bioinformatics*, 18(6): 2775-2780. <https://doi.org/10.1101/2020.02.23.20026930>
- [19] Sethy, P.K., Behera, S.K., Ratha, P.K., Biswas, P. (2020). Detection of coronavirus disease (COVID-19) based on deep features and support vector machine. *International Journal of Mathematical, Engineering and Management Sciences*, 5(4): 643-651. <https://doi.org/10.33889/IJMEMS.2020.5.4.052>
- [20] Gessert, N., Bengs, M., Wittig, L., Drömann, D., Keck, T., Schlaefer, A., Ellebrecht, D. B. (2019). Deep transfer learning methods for colon cancer classification in confocal laser microscopy images. *International Journal of Computer Assisted Radiology and Surgery*, 14(11): 1837-1845. <https://doi.org/10.1007/s11548-019-02004-1>
- [21] Dulf, E.H., Bleda, M., Mocan, T., Mocan, L. (2021). Automatic detection of colorectal polyps using transfer learning. *Sensors*, 21(17): 5704-5704. <https://doi.org/10.3390/s21175704>
- [22] Raju, M.S.N., Rao, B.S. (2022). Colorectal multi-class image classification using deep learning models. *Bulletin of Electrical Engineering and Informatics*, 11(1): 195-200. <https://doi.org/10.11591/eei.v11i1.3299>
- [23] Acar, E., Şahin, E., Yılmaz, İ. (2021). Improving effectiveness of different deep learning-based models for detecting COVID-19 from computed tomography (CT) images. *Neural Computing and Applications*, 33(24): 17589-17609. <https://doi.org/10.1007/s00521-021-06344-5>
- [24] Balasamy, K., Suganyadevi, S. (2021). A fuzzy based ROI selection for encryption and watermarking in medical image using DWT and SVD. *Multimedia Tools and Applications*, 80(5): 7167-7186. <https://doi.org/10.1007/s11042-020-09981-5>
- [25] Ngo, L., Han, J.H. (2017). Advanced deep learning for blood vessel segmentation in retinal fundus images. In 2017 5th International Winter Conference on Brain-Computer Interface (BCI), pp. 91-92. <https://doi.org/10.1109/IWW-BCI.2017.7858169>
- [26] Zhang, Q., Xiao, Y., Dai, W., Suo, J., Wang, C., Shi, J., Zheng, H. (2016). Deep learning based classification of breast tumors with shear-wave elastography. *Ultrasonics*, 72: 150-157. <https://doi.org/10.1016/j.ultras.2016.08.004>
- [27] Ouchicha, C., Ammor, O., Meknassi, M. (2020). CVDNet: A novel deep learning architecture for detection of coronavirus (Covid-19) from chest x-ray images. *Elsevier-Chaos Solitons Fractals*, 140(5): 110245-110245. <https://doi.org/10.1016/j.chaos.2020.110245>
- [28] Sethy, P.K., Behera, S.K. (2020). Detection of coronavirus disease (covid-19) based on deep features. *International Journal of Mathematical, Engineering and Management Sciences*, 5(4): 643-651. <https://doi.org/10.33889/IJMEMS.2020.5.4.052>
- [29] Jaiswal, A.K., Tiwari, P., Kumar, S., Gupta, D., Khanna, A., Rodrigues, J.J. (2019). Identifying pneumonia in chest X-rays: A deep learning approach. *Measurement*, 145: 511-518. <https://doi.org/10.1016/j.measurement.2019.05.076>
- [30] Civit-Masot, J., Luna-Perejón, F., Domínguez Morales, M., Civit, A. (2020). Deep learning system for COVID-19 diagnosis aid using X-ray pulmonary images. *Applied Sciences*, 10(13): 4640-4640. <https://doi.org/10.3390/app10134640>
- [31] Punn, N.S., Sonbhadra, S.K., Agarwal, S. (2020). COVID-19 epidemic analysis using machine learning and deep learning algorithms. *MedRxiv*. <https://doi.org/10.1101/2020.04.08.20057679>
- [32] Phillips, N.A., Rajpurkar, P., Sabini, M., et al. (2007). Chexphoto: 10,000+ smartphone photos and synthetic photographic transformations of chest x-rays for benchmarking deep learning robustness. *arXiv preprint arXiv:2007.06199*.
- [33] Raju, M.S., Rao, B.S. (2022). Colorectal cancer disease classification using Mobilenetv2 based on deep learning. *International Journal of Software Innovation (IJSI)*, 10(1): 1-18. <http://doi.org/10.4018/IJSI.309725>
- [34] Maghdid, H.S., Asaad, A.T., Ghafoor, K.Z., Sadiq, A.S., Mirjalili, S., Khan, M.K. (2021). Diagnosing COVID-19 pneumonia from X-ray and CT images using deep learning and transfer learning algorithms. In *Multimodal Image Exploitation and Learning*, 11734: 99-110. <https://doi.org/10.1117/12.2588672>
- [35] Ghoshal, B., Tucker, A. (2020). Estimating uncertainty and interpretability in deep learning for coronavirus (COVID-19) detection. *arXiv preprint arXiv:2003.10769*.
- [36] Hasan, M., Alam, M., Elahi, M., Toufick, E., Roy, S., Wahid, S.R. (2020). CVR-Net: A deep convolutional neural network for coronavirus recognition from chest radiography images. *arXiv preprint arXiv:2007.11993*.
- [37] Ker, J., Wang, L., Rao, J., Lim, T. (2017). Deep learning applications in medical image analysis. *IEEE Access*, 6: 9375-9389. <https://doi.org/10.1109/ACCESS.2017.2788044>
- [38] Litjens, G., Kooi, T., Bejnordi, B.E., et al. (2017). A survey on deep learning in medical image analysis. *Medical Image Analysis*, 42: 60-88. <https://doi.org/10.1016/j.media.2017.07.005>
- [39] Mazurowski, M.A., Buda, M., Saha, A., Bashir, M.R. (2019). Deep learning in radiology: An overview of the concepts and a survey of the state of the art with focus on MRI. *Journal of Magnetic Resonance Imaging*, 49(4): 939-954. <https://doi.org/10.1002/jmri.26534>
- [40] Pehrson, L.M., Nielsen, M.B., Ammitzbøl Lauridsen, C. (2019). Automatic pulmonary nodule detection applying deep learning or machine learning algorithms to the LIDC-IDRI database: A systematic review. *Diagnostics*, 9(1): 29-29. <https://doi.org/10.3390/diagnostics9010029>
- [41] Sengupta, S., Basak, S., Saikia, P., et al. (2020). A review of deep learning with special emphasis on architectures,

- applications and recent trends. *Knowledge-Based Systems*, 194: 105596. <https://doi.org/10.1016/j.knosys.2020.105596>
- [42] Shorten, C., Khoshgoftaar, T.M. (2019). A survey on image data augmentation for deep learning. *Journal of Big Data*, 6(1): 1-48. <https://doi.org/10.1186/s40537-019-0197-0>
- [43] Yi, X., Walia, E., Babyn, P. (2019). Generative adversarial network in medical imaging: A review. *Medical Image Analysis*, 58: 101552. <https://doi.org/10.1016/j.media.2019.101552>
- [44] Zhuang, F., Qi, Z., Duan, K., et al. (2020). A comprehensive survey on transfer learning. *Proceedings of the IEEE*, 109(1): 43-76. <https://doi.org/10.1109/JPROC.2020.3004555>
- [45] Wang, J., Zhu, H., Wang, S.H., Zhang, Y.D. (2021). A review of deep learning on medical image analysis. *Mobile Networks and Applications*, 26(1): 351-380. <https://doi.org/10.1007/s11036-020-01672-7>
- [46] Shinde, S., Kulkarni, U., Mane, D., Sapkal, A. (2021). Deep learning-based medical image analysis using transfer learning. In *Health Informatics: A Computational Perspective in Healthcare*, pp. 19-42.
- [47] Xie, X., Niu, J., Liu, X., Chen, Z., Tang, S., Yu, S. (2021). A survey on incorporating domain knowledge into deep learning for medical image analysis. *Medical Image Analysis*, 69: 101985. <https://doi.org/10.1016/j.media.2021.101985>
- [48] Wang, Y., Nazir, S., Shafiq, M. (2021). An overview on analyzing deep learning and transfer learning approaches for health monitoring. *Computational and Mathematical Methods in Medicine*, 2021: Article ID: 5552743. <https://doi.org/10.1155/2021/5552743>
- [49] Wang, S.H., Zhang, Y.D. (2020). DenseNet-201-based deep neural network with composite learning factor and precomputation for multiple sclerosis classification. *ACM Transactions on Multimedia Computing, Communications, and Applications (TOMM)*, 16(2s): 1-19. <https://doi.org/10.1145/3341095>
- [50] Acharya, U.R., Fernandes, S.L., WeiKoh, J.E., et al. (2019). Automated detection of Alzheimer's disease using brain MRI images—a study with various feature extraction techniques. *Journal of Medical Systems*, 43(9): 1-14. <https://doi.org/10.1007/s10916-019-1428-9>
- [51] Wang, S., Zhou, Q., Yang, M., Zhang, Y. (2021). ADVIAN: Alzheimer's disease VGG-inspired attention network based on convolutional block attention Module and multiple way data augmentation. *Frontiers in Aging Neuroscience*, 18(13): 313-313. <https://doi.org/10.3389/fnagi.2021.687456>
- [52] Swati, Z.N.K., Zhao, Q., Kabir, M., Ali, F., Ali, Z., Ahmed, S., Lu, J. (2019). Brain tumor classification for MR images using transfer learning and fine-tuning. *Computerized Medical Imaging and Graphics*, 75: 34-46. <https://doi.org/10.1016/j.compmedimag.2019.05.001>
- [53] Lao, J., Chen, Y., Li, Z.C., Li, Q., Zhang, J., Liu, J., Zhai, G. (2017). A deep learning-based radiomics model for prediction of survival in glioblastoma multiforme. *Scientific Reports*, 7(1): 1-8. <https://doi.org/10.1038/s41598-017-10649-8>
- [54] Puranik, M., Shah, H., Shah, K., Bagul, S. (2018). Intelligent Alzheimer's detector using deep learning. In *2018 Second International Conference on Intelligent Computing and Control Systems (ICICCS)*, pp. 318-323. <https://doi.org/10.1109/ICCONS.2018.8663065>
- [55] Cheng, B., Liu, M., Zhang, D., Shen, D. (2019). Robust multi-label transfer feature learning for early diagnosis of Alzheimer's disease. *Brain Imaging and Behavior*, 13(1): 138-153. <https://doi.org/10.1007/s11682-018-9846-8>
- [56] Lu, S., Lu, Z., Zhang, Y.D. (2019). Pathological brain detection based on AlexNet and transfer learning. *Journal of Computational Science*, 30: 41-47. <https://doi.org/10.1016/j.jocs.2018.11.008>
- [57] Sathananthavathi, V., Indumathi, G. (2021). Encoder enhanced atrous (EEA) unet architecture for retinal blood vessel segmentation. *Cognitive Systems Research*, 67: 84-95. <https://doi.org/10.1016/j.cogsys.2021.01.003>
- [58] Raju, M.S.N., Rao, B.S. (2022). Colorectal cancer disease classification and segmentation using a novel deep learning approach. *International Journal of Intelligent Engineering Systems*, 15(4): 227-236. <https://doi.org/10.22266/ijies2022.0831.21>
- [59] Chen, Y.M., Huang, W.T., Ho, W.H., Tsai, J.T. (2021). Classification of age-related macular degeneration using convolutional-neural-network-based transfer learning. *BMC Bioinformatics*, 22(5): 1-16. <https://doi.org/10.1186/s12859-021-04001-1>
- [60] Suan Ng, S., Ling Lee, H., Bothi Raja, P., Doong, R.A. (2022). Recent advances in nanomaterial-based optical biosensors as potential point-of-care testing (PoCT) probes in carcinoembryonic antigen detection. *Chemistry-An Asian Journal*, 17(14): e202200287. <https://doi.org/10.1002/asia.202200287>
- [61] Motozawa, N., An, G., Takagi, S., et al. (2019). Optical coherence tomography-based deep-learning models for classifying normal and age-related macular degeneration and exudative and non-exudative age-related macular degeneration changes. *Ophthalmology and Therapy*, 8(4): 527-539. <https://doi.org/10.1007/s40123-019-00207-y>
- [62] Tiwari, D., Dixit, M., Gupta, K. (2021). Deep multi-view breast cancer detection: A multi-view concatenated infrared thermal images based breast cancer detection system using deep transfer learning. *Traitement du Signal*, 38(6): 1699-1711. <https://doi.org/10.18280/ts.380613>
- [63] Moroiianu, S.L., Rusu, M. (2021). Detecting invasive breast carcinoma on dynamic contrast-enhanced MRI. In *Medical Imaging 2021: Computer-Aided Diagnosis*, 11597: 95-101. <https://doi.org/10.1117/12.2580989>
- [64] Mendel, K., Li, H., Sheth, D., Giger, M. (2019). Transfer learning from convolutional neural networks for computer-aided diagnosis: a comparison of digital breast tomosynthesis and full-field digital mammography. *Academic Radiology*, 26(6): 735-743. <https://doi.org/10.1016/j.acra.2018.06.019>
- [65] Aljuaid, H., Alturki, N., Alsubaie, N., Cavallaro, L., Liotta, A. (2022). Computer-aided diagnosis for breast cancer classification using deep neural networks and transfer learning. *Computer Methods and Programs in Biomedicine*, 223: 106951. <https://doi.org/10.1016/j.cmpb.2022.106951>
- [66] Islam, W., Jones, M., Faiz, R., Sadeghipour, N., Qiu, Y., Zheng, B. (2022). Improving performance of breast lesion classification using a ResNet50 model optimized with a novel attention mechanism. *Tomography*, 8(5): 2411-2425. <https://doi.org/10.3390/tomography8050200>
- [67] Byra, M., Sznajder, T., Korzinek, D., Piotrkowska-Wróblewska, H., Dobruch-Sobczak, K., Nowicki, A.,

- Marasek, K. (2019). Impact of ultrasound image reconstruction method on breast lesion classification with deep learning. In Iberian Conference on Pattern Recognition and Image Analysis, pp. 41-52. https://doi.org/10.1007/978-3-030-31332-6_4
- [68] Li, X., Shen, X., Zhou, Y., Wang, X., Li, T.Q. (2020). Classification of breast cancer histopathological images using interleaved DenseNet with SENet (IDSNet). *PloS One*, 15(5): e0232127. <https://doi.org/10.1371/journal.pone.0232127>
- [69] Gessert, N., Bengs, M., Wittig, L., Drömann, D., Keck, T., Schlaefer, A., Ellebrecht, D.B. (2019). Deep transfer learning methods for colon cancer classification in confocal laser microscopy images. *International Journal of Computer Assisted Radiology and Surgery*, 14(11): 1837-1845. <https://doi.org/10.1007/s11548-019-02004-1>
- [70] Dulf, E.H., Bleda, M., Mocan, T., Mocan, L. (2021). Automatic detection of colorectal polyps using transfer learning. *Sensors*, 21(17): 5704-5704. <https://doi.org/10.3390/s21175704>
- [71] Shafiei, F., Fekri-Ershad, S. (2020). Detection of lung cancer tumor in CT scan images using novel combination of super pixel and active contour algorithms. *Traitement du Signal*, 37(6): 1029-1035. <https://doi.org/10.18280/ts.370615>
- [72] Kang, J., Gwak, J. (2019). Ensemble of instance segmentation models for polyp segmentation in colonoscopy images. *IEEE Access*, 7: 26440-26447. <https://doi.org/10.1109/ACCESS.2019.2900672>
- [73] Zhang, S., Sun, F., Wang, N., et al. (2019). Computer-aided diagnosis (CAD) of pulmonary nodule of thoracic CT image using transfer learning. *Journal of Digital Imaging*, 32(6): 995-1007. <https://doi.org/10.1007/s10278-019-00204-4>
- [74] Xiong, J., Li, X., Lu, L., Schwartz, L.H., Fu, X., Zhao, J., Zhao, B. (2019). Implementation strategy of a CNN model affects the performance of CT assessment of EGFR mutation status in lung cancer patients. *IEEE Access*, 7: 64583-64591. <https://doi.org/10.1109/ACCESS.2019.2916557>
- [75] Hussein, S., Kandel, P., Bolan, C.W., Wallace, M.B., Bagci, U. (2019). Lung and pancreatic tumor characterization in the deep learning era: novel supervised and unsupervised learning approaches. *IEEE Transactions on Medical Imaging*, 38(8): 1777-1787. <https://doi.org/10.1109/TMI.2019.2894349>
- [76] Zhang, D., Han, J., Cheng, G., Yang, M.H. (2021). Weakly supervised object localization and detection: A survey. *IEEE Transactions on Pattern Analysis and Machine Intelligence*, 44(9): 5866-5885. <https://doi.org/10.1109/TPAMI.2021.3074313>
- [77] da Nóbrega, R.V.M., Rebouças Filho, P.P., Rodrigues, M. B., da Silva, S.P., Dourado Júnior, C.M., de Albuquerque, V.H.C. (2020). Lung nodule malignancy classification in chest computed tomography images using transfer learning and convolutional neural networks. *Neural Computing and Applications*, 32(15): 11065-11082. <https://doi.org/10.1007/s00521-018-3895-1>
- [78] Bassi, P.R., Attux, R. (2022). A deep convolutional neural network for COVID-19 detection using chest X-rays. *Research on Biomedical Engineering*, 38(1): 139-148. <https://doi.org/10.1007/s42600-021-00132-9>
- [79] Wu, F., Zhao, S., Yu, B., et al. (2020). A new coronavirus associated with human respiratory disease in China. *Nature*, 579(7798): 265-269. <https://doi.org/10.1038/s41586-020-2008-3>
- [80] economist.com, 2020. Academic articles, <https://www.economist.com/graphic-detail/2020/03/20/coronavirus-research-is-being-published-at-a-furious-pace>, accessed on 12 June 2022.
- [81] Hassaballah, M., Awad, A.I. (Eds.). (2020). *Deep Learning in Computer Vision: Principles and Applications*. CRC Press.
- [82] Ciaparrone, G., Sánchez, F.L., Tabik, S., Troiano, L., Tagliaferri, R., Herrera, F. (2020). Deep learning in video multi-object tracking: A survey. *Neurocomputing*, 381: 61-88. <https://doi.org/10.1016/j.neucom.2019.11.023>
- [83] Elharrouss, O., Almaadeed, N., Al-Maadeed, S. (2020). An image steganography approach based on k-least significant bits (k-LSB). In *2020 IEEE International Conference on Informatics, IoT, and Enabling Technologies (ICIOT)*, pp. 131-135. <https://doi.org/10.1109/ICIOT48696.2020.9089566>
- [84] Shankar, K., Zhang, Y., Liu, Y., Wu, L., Chen, C.H. (2020). Hyperparameter tuning deep learning for diabetic retinopathy fundus image classification. *IEEE Access*, 8: 118164-118173. [10.1109/ICIOT48696.2020.9089566](https://doi.org/10.1109/ICIOT48696.2020.9089566)
- [85] Li, F., Liu, Z., Chen, H., Jiang, M., Zhang, X., Wu, Z. (2019). Automatic detection of diabetic retinopathy in retinal fundus photographs based on deep learning algorithm. *Translational Vision Science & Technology*, 8(6): 4-4. <https://doi.org/10.1167/tvst.8.6.4>